



# UNIVERSITÀ DI PARMA

## ARCHIVIO DELLA RICERCA

University of Parma Research Repository

Conservative management in a case of iatrogenic twin anemia-polycythemia sequence.

This is the peer reviewed version of the following article:

*Original*

Conservative management in a case of iatrogenic twin anemia-polycythemia sequence / Fratelli, N; Prefumo, F; Zambolo, C; Zanardini, C; Fichera, A; Frusca, Tiziana. - In: ULTRASOUND IN OBSTETRICS & GYNECOLOGY. - ISSN 0960-7692. - 39:(2012), pp. 597-597. [10.1002/uog.10135]

*Availability:*

This version is available at: 11381/2681525 since: 2016-10-06T16:33:10Z

*Publisher:*

*Published*

DOI:10.1002/uog.10135

*Terms of use:*

Anyone can freely access the full text of works made available as "Open Access". Works made available

*Publisher copyright*

note finali coverpage

(Article begins on next page)



# Letters to the Editor

## Teaching and learning normal gynecological ultrasonography using simple virtual reality objects: a proposal for a standardized approach

Teaching basic gynecological and obstetric ultrasonography remains a challenge<sup>1</sup>; it typically consists of limited personal instruction by an expert while a patient, having agreed to a ‘training exam’, is being scanned. Virtual reality object movies displaying both normal and abnormal anatomy in a simple interactive format have recently been proposed for obstetric ultrasound teaching<sup>2,3</sup>. We here extend virtual reality object movies to imaging of the normal female anatomy as it is seen in abdominal and vaginal ultrasound images and combine the resulting interactive material with an anatomical teaching approach demonstrating how to obtain diagnostic images in gynecological patients.

Sonographic volume datasets from different insonation routes and angles were digitally sectioned in optimized orientations so that the sections obtained correspond to typical diagnostic planes in realtime scanning (Movies S1–S24). Table 1 lists the insonation routes, probe positioning and orientation landmarks for the provided object movies. Figure 1 shows key frames from a normal female pelvis with annotation of the most important anatomical landmarks, while Figure S1 shows the principal positions of the transvaginal probe, used to acquire the datasets, which may serve as reference positions when examining a patient. Figure 2 shows correlation of the principal vaginal probe orientations

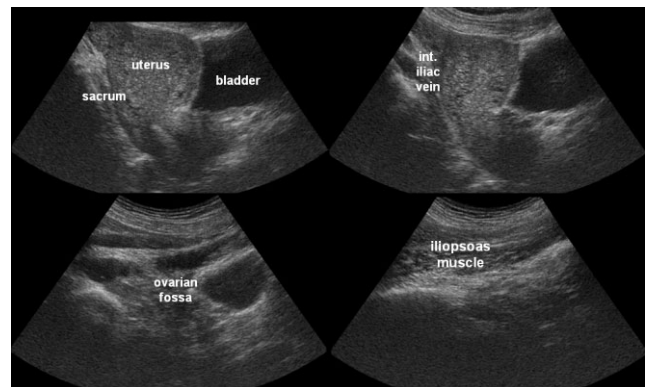


**Figure 1** Sample image sequence used for construction of a virtual reality object movie. The parallel sagittal sections, obtained using transabdominal ultrasound, show representative images from one virtual reality object (virtual reality object Movie S1) with annotations of the most prominent anatomical landmarks of a normal female pelvis.

with the corresponding ultrasound images. Figures S2 and S3 show characteristic still images taken from the virtual reality object movies for transabdominal and transvaginal imaging, respectively, with annotations.

Ultrasonography is considered by many practicing gynecologists to be their major diagnostic tool. This applies in particular to a transvaginal probe, which can be brought much closer to the object of interest (uterus, ovaries, Fallopian tubes) and usually has excellent resolution owing to its higher frequencies. But teaching transvaginal scanning poses unique challenges. Firstly, most women consider a vaginal ultrasound exam as at

**Table 1** Insonation routes and probe positioning used for obtaining volume datasets contained in the virtual reality movies. These proposed anatomically oriented insonation approaches can also be used as a standardized approach for teaching gynecological ultrasonography. Transabdominal imaging as suggested will yield typical images as shown in Figure 1. Principal movements of the vaginal probe are depicted in Figure S1. Figure 2 shows correlation of the probe positioning required to visualize the pelvic walls with the resulting ultrasound images

<i>Insonation route</i>	<i>Probe position</i>	<i>Orientation landmarks typically seen using this approach</i>
Transabdominal	Median longitudinal	Maximum sagittal diameter of the bladder, usually a median section of the uterus
	Paramedian longitudinal (on the right or left side, just medial to the pelvic bone)	Longitudinal section of the external iliac vessels
Transvaginal	Axially inserted into the vagina, just inside the introitus	Hypoechoic image of urethra and paraurethral tissue, rectal mucosa and muscular layers
	Axially inserted into the vagina, the probe just in contact with the portio uteri; depending on the presence of uterine anteversion or retroflexion: lower or raise probe handle to view more anteriorly or posteriorly	Uterine cervix and endocervical canal
	Axially inserted into the vagina, turned towards the right (or left) pelvic wall and rotated about 50° counterclockwise (or clockwise)	Pelvic wall with a longitudinal section of the external iliac vessels and often the normally positioned right (or left) ovary
	Axially inserted into the vagina, turned towards the right (or left) pelvic wall and rotated about 90° counterclockwise (or clockwise), to try to obtain the ipsilateral ovary and an oblique section of the uterus in one image	Ovary, Fallopian tube with its prominent vessels and oblique section of the uterus

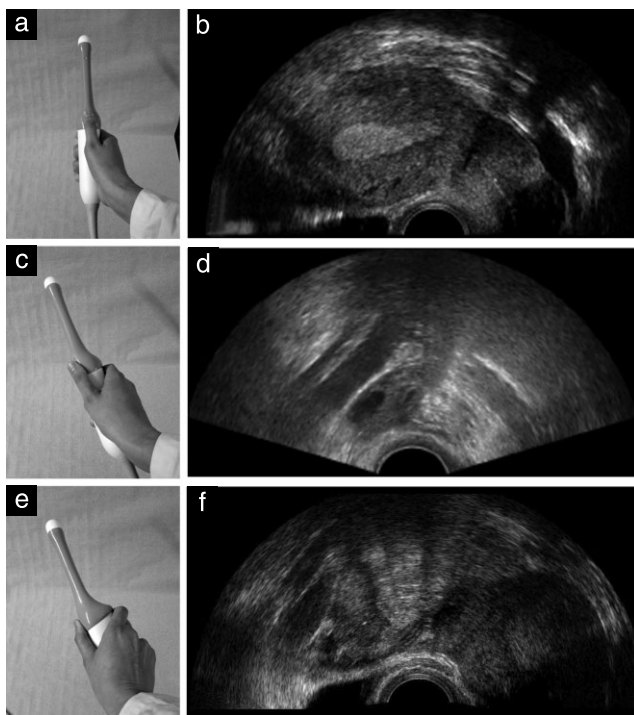


**Figure 2** Vaginal probe orientation and resulting ultrasound images. Shown are the starting ultrasound images of the virtual reality object Movies S10, S16 and S20, respectively. (a,b) Neutral positioning of the probe, resulting in a median longitudinal section of the uterus; (c,d) pointing the transducer to the right of the patient and rotating it counterclockwise gives a display of the right external iliac vessels and often the right ovary; (e,f) further rotation from the orientation shown in (c) and (d) typically gives an oblique section of the uterus, the Fallopian tube and the ovary.

least uncomfortable. This applies even more to a teaching situation in which an experienced examiner guides a trainee. Secondly, in contrast to abdominal ultrasound scanning, the maneuvers available to position the probe relative to the object to be studied are limited: insertion of the probe into the vagina in the axial direction, lowering and raising of the probe handle to direct the beam anteriorly or posteriorly, tilting towards the pelvic walls and rotating the probe around its long axis. These obstacles prevent many interested trainees from acquiring the diagnostic confidence found in expert centers.

Virtual reality movies simulate an 'ideal' ultrasound scan in that they allow the operator to move through the female pelvis in standard orientations, identify the correct plane and demonstrate the relevant findings. They are intuitive to use, easy to operate, extremely economic in terms of the digital storage space they occupy and can easily be shared. These advantages and their interactivity make them also the perfect tools for online teaching.

More complex simulators, addressing in addition handling and positioning of ultrasound probes (transabdominal or transvaginal), have also been developed and used for gynecological ultrasonography<sup>4–10</sup>. Yet, the required

hardware and cost seem to have precluded widespread use of such systems.

The virtual reality objects presented here do not allow correlation of probe movement with the sections displayed on the screen; this movement is emulated using a standard computer pointing device. Another limitation of our approach is that orientation of the stack of planes accessible in the virtual reality object is fixed. The orientation of the current virtual reality objects (vaginal probe on the bottom of the monitor, bladder to the left) can easily be changed by electronically inverting the virtual reality objects (see object Movie S24).

For those responsible for training in gynecological ultrasound, our material may form the basis for a practical component of a basic program. Of course, this approach can be extended to produce a digital library of typical gynecological anomalies (for example uterine tumors, adnexal tumors or uterine anomalies) that can be diagnosed by ultrasound.

B. Tutschek\*†‡, S. Tercanli† and F. Chantraine§  
 †Center for Fetal Medicine and Women's Ultrasound,  
 Freie Strasse 38, 4001 Basel, Switzerland; ‡Medical  
 Faculty, Heinrich Heine University, Düsseldorf,  
 Germany; §Obstetrics and Gynecology, University  
 Hospital Liege, Belgium  
 \*Correspondence.  
 (e-mail: tutschek@uni-duesseldorf.de)

DOI: 10.1002/uog.11090

## References

- Salvesen KA, Lees C, Tutschek B. Basic European ultrasound training in obstetrics and gynecology: where are we and where do we go from here? *Ultrasound Obstet Gynecol* 2010; **36**: 525–529.
- Tutschek B. Simple virtual reality display of fetal volume ultrasound. *Ultrasound Obstet Gynecol* 2008; **32**: 906–909.
- Tutschek B, Pilu G. Virtual reality ultrasound imaging of the normal and abnormal fetal central nervous system. *Ultrasound Obstet Gynecol* 2009; **34**: 259–267.
- Lee W, Ault H, Kirk JS, Comstock CH. Interactive multimedia for prenatal ultrasound training. *Obstet Gynecol* 1995; **85**: 135–140.
- Meller G. A typology of simulators for medical education. *J Digit Imaging* 1997; **10**: 194–196.
- Meller G, Tepper R, Bergman M, Anderhub B. The tradeoffs of successful simulation. *Stud Health Technol Inform* 1997; **39**: 565–571.
- Smith JF Jr, Bergmann M, Gildersleeve R, Allen R. A simple model for learning stereotactic skills in ultrasound-guided amniocentesis. *Obstet Gynecol* 1998; **92**: 303–305.
- Baier P, Scharf A, Sohn C. [New ultrasound simulation system: a method for training and improved quality management in ultrasound examination]. *Z Geburtshilfe Neonatol* 2001; **205**: 213–217.
- Advanced medical simulation. www.medsim.com [accessed 1 September 2011].
- Ultraschall-Simulatoren für die Medizin. www.sonofit.de [accessed 1 September 2011].

## SUPPORTING INFORMATION ON THE INTERNET

The following supporting information may be found in the online version of this article:

 **Figures S1–S3** Still images showing probe handling, insonation directions and characteristic images obtained using transabdominal and transvaginal ultrasound

**Movies S1–S24** QuickTime virtual reality object movies exemplifying the standardized approach to gynecological ultrasound examination outlined in Table 1, with normal findings and some common abnormal findings demonstrated. Note, QuickTime version 7, which can be downloaded from [apple.com/quicktime/download](http://apple.com/quicktime/download), is required to view these movies.

**ovary, tube and uterus (tilted view).zip** This compressed file, as an example, contains the volume data set of Movie S20 in an alternative viewing format, Adobe Flash®. To display this object movie, unzip the three files contained in the .zip file then open the extracted HTML file in a browser.

**PDF Slide with Videos.zip** This compressed file contains a PDF illustrating examination technique for transvaginal ultrasound with hyperlinks to relevant movie objects.

## Conservative management in a case of iatrogenic twin anemia–polycythemia sequence

We read with interest the recent article by Groussolles *et al.*<sup>1</sup> describing the management of a case of twin anemia–polycythemia sequence (TAPS). Different treatments for TAPS have been suggested<sup>2–4</sup>.

A 32-year-old woman, gravida 2 para 1, with a monochorionic–diamniotic twin pregnancy complicated by Quintero stage III twin-to-twin transfusion syndrome (TTTS)<sup>5</sup> was referred to Brescia University Hospital at 24 + 2 weeks' gestation for laser treatment. Weekly sonographic surveillance after the procedure confirmed complete regression of TTTS. However, TAPS was suspected at 27 + 0 weeks<sup>6</sup>. The former recipient twin became polycythemic, with a middle cerebral artery peak systolic velocity (MCA-PSV) < 1 multiple of the median (MoM) (26 cm/s (0.73 MoM)), and the former donor became anemic, with an MCA-PSV > 1.5 MoM (55 cm/s (1.56 MoM)). One week later the clinical picture was similar. Different management options were discussed with the patient and in view of the gestational age and the apparently slow progression of the disease we opted for expectant management.

Longitudinal measurement of MCA-PSV confirmed the slow progression of the disease. At 32 + 1 weeks the MCA-PSV was 61 cm/s (1.37 MoM) in the anemic twin and 21 cm/s (0.47 MoM) in the polycythemic twin. Elective Cesarean delivery was performed at 32 + 3 weeks after maternal administration of steroids. The previous donor (1490 g) was anemic (hemoglobin (Hb) 5 g/dL, hematocrit 16%) and required neonatal blood transfusions, the previous recipient (1678 g) was polycythemic (Hb 24 g/dL, hematocrit 76%) and required partial exchange transfusions. Placental study performed with milk injection showed a small arteriovenous anastomosis missed at the time of laser treatment. Postnatal ultrasound excluded cerebral hemorrhage in both twins. The previous recipient had an uncomplicated hospitalization and was discharged after 24 days. The previous donor required prolonged ventilatory support and right inguinal hernia repair. He was discharged after 75 days with mild hypotonia and needed oxygen support.

In cases of TAPS, laser ablation of residual anastomoses can be difficult because of absence of polyhydramnios, less clear amniotic fluid, absence of a 'stuck twin' and need for amnioinfusion<sup>1,4</sup>. Recurrent anemia in the donor due to the persistence of blood loss through arteriovenous anastomoses and hyperviscosity syndrome in the recipient are well known complications of TAPS treated by intrauterine transfusions. Moreover repeat transfusions potentially increase the risk of procedure-related complications<sup>2</sup>. Considering the slow progression of the disease, in our case we opted for conservative management with elective Cesarean delivery beyond 32 + 0 weeks' gestation. Even if no definitive conclusions can be drawn regarding the optimal treatment of severe TAPS, our report highlights the need for routine assessment of MCA-PSV in monochorionic pregnancies, in order to detect spontaneous or iatrogenic TAPS and allow tailored management.

N. Fratelli\*†, F. Prefumo‡, C. Zambolo‡,  
C. Zanardini‡, A. Fichera‡ and T. Frusca‡  
†Department of Obstetrics and Gynaecology,  
Sacro Cuore Don Calabria General Hospital,  
Negrar (VR), Italy; ‡Maternal Fetal Medicine Unit,  
University of Brescia, Brescia, Italy  
\*Correspondence.  
(e-mail: nicolaf23@gmail.com)

DOI: 10.1002/uog.10135

## References

- Groussolles M, Sartor A, Connan L, Vayssière C. Evolution of middle cerebral artery peak systolic velocity after a successful laser procedure for iatrogenic twin anemia–polycythemia sequence. *Ultrasound Obstet Gynecol* 2012; **39**: 354–356.
- Robyr R, Lewi L, Salomon LJ, Yamamoto M, Bernard JP, Deprest J, Ville Y. Prevalence and management of late fetal complications following successful selective laser coagulation of chorionic plate anastomoses in twin-to-twin transfusion syndrome. *Am J Obstet Gynecol* 2006; **194**: 796–803.
- Herway C, Johnson A, Moise K, Moise KJJ. Fetal intraperitoneal transfusion for iatrogenic twin anemia–polycythemia sequence

- after laser therapy. *Ultrasound Obstet Gynecol* 2009; 33: 592–594.
4. Weingartner AS, Kohler A, Kohler M, Bouffet N, Hunsinger MC, Mager C, Hornecker F, Neumann M, Schmerber E, Tanghe M, Viville B, Favre R. Clinical and placental characteristics in four new cases of twin anemia–polycythemia sequence. *Ultrasound Obstet Gynecol* 2010; 35: 490–494.
  5. Quintero RA, Morales WJ, Allen MH, Bornick PW, Johnson PK, Kruger M. Staging of twin–twin transfusion syndrome. *J Perinatol* 1999; 19: 550–555.
  6. Slaghekke F, Kist WJ, Oepkes D, Pasman SA, Middeldorp JM, Klumper FJ, Walther FJ, Vandenbussche FP, Lopriore E. Twin anemia-polycythemia sequence: diagnostic criteria, classification, perinatal management and outcome. *Fetal Diagn Ther* 2010; 27: 181–190.

### Ductus venosus blood-flow patterns: more than meets the eye?

The Doppler evaluation of fetal venous flow-velocity waveforms is of clinical relevance in conditions that are associated with cardiovascular manifestations. In contrast to arterial flow, velocity waveform characteristics of the venous-flow profile relate to atrial pressure and volume changes throughout the entire cardiac cycle, producing a multiphasic flow pattern<sup>1</sup>. Among the fetal venous vessels, the ductus venosus has a special role because its flow is under active regulation and its anatomy results in a flow-velocity profile that is typically antegrade throughout the entire cardiac cycle and, therefore, lends itself to qualitative assessment<sup>1,2</sup>.

Designation of the individual phases of the venous flow-velocity waveform is based on the timing of the cardiac cycle. With the initiation of ventricular systole the descent of the atrioventricular (AV) valve ring decreases atrial pressure and increases the amount of venous return that can be accommodated by the atria. This produces the first increase in venous forward velocities, which peak at the S-wave. As the ventricle relaxes in the second half of systole the AV valve ring ascends towards its resting position, atrial pressures rise and venous forward velocities fall to the first trough, designated as the v-descent. Once ventricular relaxation is complete, the higher pressures in the atria lead to an opening of the AV valves, allowing for an increase in venous forward velocities towards the second peak during passive diastolic ventricular filling (D-wave). With the discharge of the sinoatrial node, atrial contraction initiates active ventricular diastolic filling and produces a sharp increase in atrial pressures. The fall in venous forward velocities produces the second trough, designated the a-wave (Figure 1).

There are several variables including afterload, cardiac contractility, compliance and vascular volume that can affect cardiac function and therefore intra-atrial pressure–volume relationships. Because of the timing of events during the cardiac cycle, individual aspects of myocardial dysfunction may be more apparent during specific phases of the venous flow-velocity waveform (Figure 1). Accordingly, increased afterload or decreased cardiac contractility may affect S-wave velocities, as well

as D and a-wave velocities, because of the increase in end-systolic ventricular volumes that may impair diastolic ventricular filling. In contrast, abnormalities in ventricular relaxation, an oxygen-dependent process in the fetus, may predominantly affect the v-descent. Restriction to ventricular filling, either by extracardiac compression or decreased cardiac compliance, is more likely to affect the D- and a-waves. Finally, restriction to atrial systolic emptying, for example due to valvular disease, may have its predominant effect during atrial systole. The association of specific cardiac functional abnormalities with characteristic patterns of the jugular venous pulse has been long recognized in adult medicine<sup>3</sup>. But while more sophisticated direct measurements of cardiac functional variables have replaced clinical evaluation in adult medicine not all of these techniques are available for examination of the human fetus.

Our primary assessment of the ductus venosus flow velocity waveform is by Doppler indices that predominantly reflect S/a and to a lesser degree D/a and S/D velocity relationships, or by qualitative analysis focusing on the a-wave<sup>4–6</sup>. There is increasing evidence that such assessment has limitations in assessing the primary underlying cardiac functional component when the Doppler index is elevated. During the construction of reference ranges it has been recognized that diastolic AV waveforms do not relate to ductus venosus or inferior vena cava peak velocity or pulsatility index (PIV)<sup>7</sup>. During simultaneous evaluation of placental and venous Doppler measurements we realized that afterload has the greatest impact on the ductus venosus PIV and the

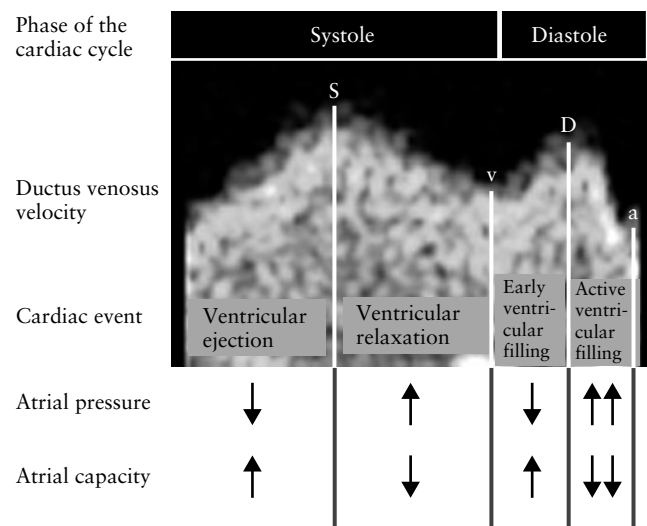


**Figure 1** Representation of the major cardiac events that coincide with the four phases of the ductus venosus flow-velocity waveform. The S-wave (S) and v-descent (v) occur during ventricular systole and the D-wave (D) and a-wave (a) during ventricular diastole. During descent of the atrioventricular valve ring with ventricular contraction, atrial pressures fall and capacity is increased, resulting in increased forward velocities. During ventricular relaxation this process reverses, producing the v-descent. During early passive ventricular filling, atrial pressure falls and capacity rises. With atrial systole there is a sharp rise in atrial pressure and a decrease in capacity, producing a corresponding decrease in forward velocity.

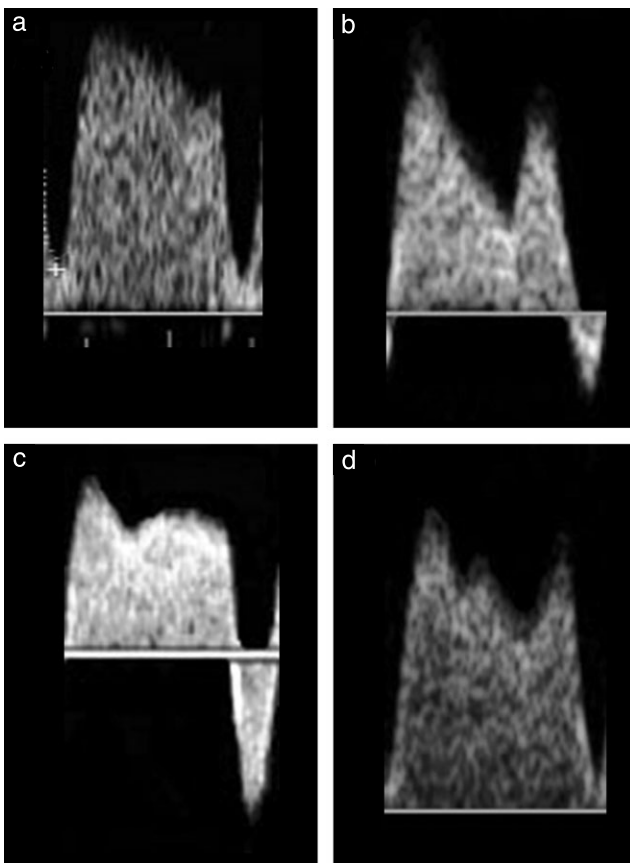


**Figure 2** Abnormal ductus venosus waveforms in fetuses with different underlying causes. (a) Recipient twin in twin–twin transfusion syndrome at 22 weeks' gestation, showing a predominant decrease in a-wave velocities and, to a lesser degree, of D-wave velocities. (b) A growth-restricted fetus at 28 weeks' gestation, showing reduced v-descent and loss of the smooth waveform contour, giving it an 'M' shape. (c) A 29-week fetus with Ebstein anomaly, showing marked reversal of the a-wave, which is comparable with the 'cannon a-wave' described in adult medicine. (d) A fetus with cardiomyopathy secondary to maternal Sjögren syndrome, showing visual asynchrony between left and right ventricular relaxation potentially contributing to the tetraphasic pattern with two troughs during v-descent.

least impact on the inferior vena cava S/a ratio<sup>6</sup>. In fetal growth restriction (FGR) it is known that high placental afterload, myocardial dysfunction and ductus venosus dilatation can all be associated with abnormal index elevation<sup>8</sup>. Accordingly, global myocardial dysfunction is not universally present in all cases of FGR with elevated ductus venosus Doppler index<sup>9</sup>. These observations raise the possibility that ductus venosus waveform analysis as it is currently practiced potentially provides insufficient or misleading information on the nature of cardiovascular compromise in various fetal conditions.

During the management of various fetal conditions we have noticed several types of ductus venosus waveform abnormalities<sup>10</sup>. A familiar type of waveform abnormality is decreased forward velocity during atrial systole and during the D-wave (Figure 2a). In some fetuses we notice an abnormally low v-descent, sometimes as low as the a-wave. This is often associated with loss of the typically smooth contour of the venous flow profile, resulting in

an 'M' shaped waveform (Figure 2b). In patients with obstructive AV valve disease we have observed marked reversal of the a-wave of a magnitude comparable with that of the D-wave (Figure 2c). Finally, in a small number of fetuses with visually asynchronous left and right ventricular relaxation we have observed a tetraphasic waveform pattern (Figure 2d). These differences in waveform abnormalities suggest the possibility of different underlying mechanisms. Evaluation of this possibility requires a departure from the current semiquantitative waveform analysis to a more systematic evaluation of the relationships between the individual phases of the ductus venosus waveform and direct measurements of related cardiovascular variables. The aim of this Letter is to suggest that such detailed venous waveform analysis is likely to provide greater insight into the pathophysiology of many fetal conditions, with a potential for greater discrimination in assessment and improvements in management.

A. A. Baschat\*, O. M. Turan and S. Turan  
*Department of Obstetrics, Gynecology and Reproductive Sciences, University of Maryland, 22 South Greene Street, 6<sup>th</sup> floor, 6NE12 Baltimore, MD 21201, USA*

\*Correspondence.

(e-mail: aabaschat@hotmail.com)

DOI: 10.1002/uog.10151

## References

1. Baschat AA, Harman CR. Venous Doppler in the assessment of fetal cardiovascular status. *Curr Opin Obstet Gynecol* 2006; **18**: 156–163.
2. Kiserud T. Physiology of the fetal circulation. *Semin Fetal Neonat Med* 2005; **10**: 493–503.
3. Pappworth MH. *A primer of Medicine* (5<sup>th</sup> edn). Butterworth-Heinemann Ltd: London, 1984.
4. Rizzo G, Capponi A, Talone PE, Arduini D, Romanini C. Doppler indices from inferior vena cava and ductus venosus in predicting pH and oxygen tension in umbilical blood at cordocentesis in growth-retarded fetuses. *Ultrasound Obstet Gynecol* 1996; **7**: 401–410.
5. Baschat AA, Güclü S, Kush ML, Gembruch U, Weiner CP, Harman CR. Venous Doppler in the prediction of acid–base status of growth-restricted fetuses with elevated placental blood flow resistance. *Am J Obstet Gynecol* 2004; **191**: 277–284.
6. Baschat AA. Relationship between placental blood flow resistance and precordial venous Doppler indices. *Ultrasound Obstet Gynecol* 2003; **22**: 561–566.
7. Hecher K, Campbell S, Snijders R, Nicolaidis K. Reference ranges for fetal venous and atrioventricular blood flow parameters. *Ultrasound Obstet Gynecol* 1994; **4**: 381–390.
8. Bellotti M, Pennati G, De Gasperi C, Bozzo M, Battaglia FC, Ferrazzi E. Simultaneous measurements of umbilical venous, fetal hepatic, and ductus venosus blood flow in growth-restricted human fetuses. *Am J Obstet Gynecol* 2004; **190**: 1347–1358.
9. Cruz-Martinez R, Figueras F, Benavides-Serralde A, Crispi F, Hernandez-Andrade E, Gratacos E. Sequence of changes in myocardial performance index in relation to aortic isthmus and ductus venosus Doppler in fetuses with early-onset intrauterine growth restriction. *Ultrasound Obstet Gynecol* 2011; **38**: 179–184.
10. Turan S, Turan OM, Monagle K, Baschat AA. OC245: Going beyond the Doppler index: a clinical classification of abnormal ductus venosus (DV) blood flow. *Ultrasound Obstet Gynecol* 2007; **30** (Suppl.): 442.